



## Infrared Spectrograph Technical Report Series

# IRS-TR 04002: Discontinuities between the Low-Resolution Modules on the IRS

G. C. Sloan \*

9 April, 2004

### Abstract

Many observers have found an abrupt jump in their spectra from the IRS at the boundary between Short-Low and Long-Low. This report analyzes these discontinuities in 86 observations of standard stars from Campaigns P, 1, 2, and 3. A discontinuity is defined here as the ratio of the measured flux in SL over LL (SL/LL) between 14.0 and 14.3  $\mu\text{m}$ . The mean discontinuity is 0.96. The distribution of discontinuities has a standard deviation of 9% about this mean, but it is not symmetric, with a sharp boundary at  $\text{SL/LL} = 1.06$  and a gradual decline to lower values of  $\text{SL/LL}$ . In the sample investigated, the lowest value is 0.58, but for fainter or redder sources the minimum may drop further. Analysis of these discontinuities using a previously developed model of spectral pointing-induced throughput error (SPITE) produces pointing offsets larger than expected, suggesting that either random pointing offsets are not responsible for the discontinuities or some systematic pointing error is responsible.

## 1 Introduction

The issue of discontinuities between spectra taken in different apertures with the Infrared Spectrograph (IRS) on the Spitzer Space Telescope has grown significant

---

\*Infrared Spectrograph Science Center, Cornell University

as observers attempt to understand and analyze their spectroscopic data. This report approaches the problem by investigating observations of all standard stars observed in Campaigns P, 1, 2, and 3, and it focuses on the discontinuity between SL1 (7.5–14.3  $\mu\text{m}$ ) and LL2 (14.0–20.7  $\mu\text{m}$ ). This set of data represents 86 AORs and should provide a good statistical basis for defining the problem.

## 2 Analysis

All spectra were processed in the following manner:

- (1) The starting point is the `bcd_fp.fits` files produced by the SSC online pipeline (version S9.1).
- (2) All images were differenced to subtract the background. SL images were differenced, DCE by DCE, with the corresponding image in the other aperture (i.e. SL1–SL2 and vice versa). LL images were differenced similarly, except that the two nods in each aperture were subtracted from each other.
- (3) Spectra were extracted using the offline pipeline (version S9.1, as mirrored at Cornell). The programs *profile* and *ridge* were applied to undifferenced images, while the extractions were made (with *extract*) from differenced images. The default field-of-view files were used. A spectrum was extracted from each DCE.
- (4) Spectra were calibrated using vector corrections for each nod position and aperture (SL2, SL1, LL2, LL1) developed by comparing the standard stars HR 6348 (K0 III), HD 173511 (K4 III) and HD 166780 (K5 III) to their spectral templates. For both LL2 and LL1, the resulting ratios for all three stars were averaged together. For both SL2 and SL1, the star HR 6348 was used as the sole standard in order to avoid complications from the CO and SiO bands at 5 and 8  $\mu\text{m}$  (these are deeper in the later-type K giants). The observations of HR 6348 were not centered in the slit, so the individual DCEs were corrected using scalar multipliers determined by comparison to HD 173511 and HD 166780.
- (5) Extracted and corrected spectra for a given aperture in each AOR were then coadded into a single spectrum, resulting in separate calibrated spectra for SL2, SL1, LL2, and LL1. The eight stars discussed here which were observed in IRS-070 in Campaign P were observed in two identical and sequential AORs, which were combined together into a single spectrum. With this exception, the AORS from other activities in Campaign P and from the campaigns during normal operations (1–3) are treated independently. This reduces the number of independent spectra from 86 to 78.
- (6) The spectra from all four apertures for each AOR were combined into one

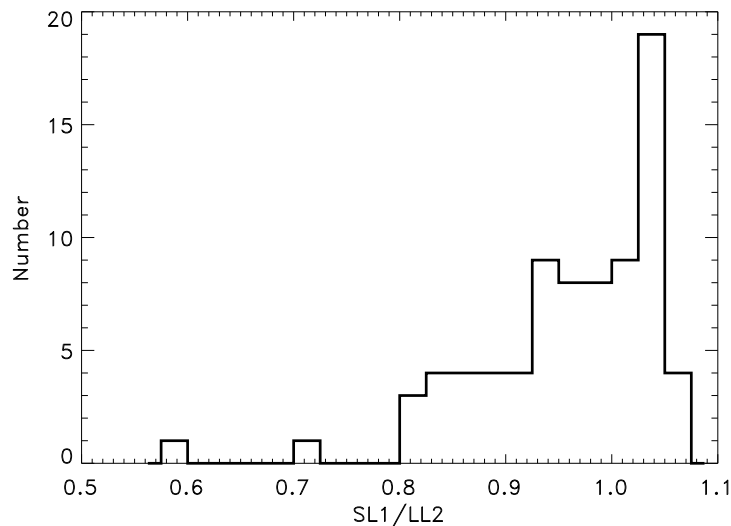


Figure 1 — The distribution of observations as a function of the discontinuity SL1/LL2. The average ratio  $SL1/LL2 = 0.958 \pm 0.087$ . The distribution is decidedly non-Gaussian.

spectrum without making any correction for discontinuities between spectral segments.

(7) The discontinuity at the interface between SL1 and LL2 is measured by summing the flux from the respective apertures in the range 14.0–14.3  $\mu\text{m}$ . This measurement is expressed as the ratio SL1/LL2.

## 3 Results

### 3.1 General Distribution

Examining the sample as a whole reveals that the average discontinuity, expressed as the ratio SL1/LL2, is  $0.958 \pm 0.087$ . Figure 1 illustrates how the discontinuities are distributed. The average would change if the calibration of SL1 relative to LL2 changed, but the standard deviation would not. In other words, *one can calibrate away the mean discontinuity, but not the spread in discontinuities*.

Of the 78 spectra counted, 44 (56%) show discontinuities in the range  $\pm 5\%$  (using this particular calibration), and 61 (78%) are within  $\pm 10\%$ . Thus 22% of the sample lie outside the range  $\pm 10\%$ .

The distribution of discontinuities is not Gaussian. The distribution is peaked

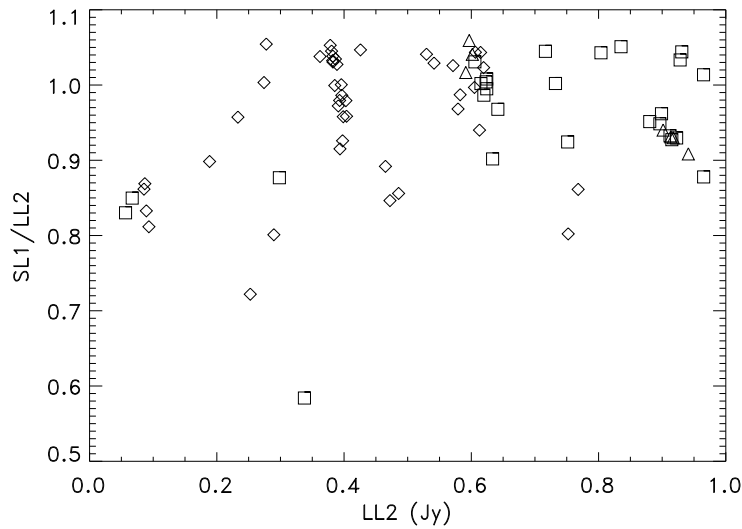


Figure 2 — The strength of the discontinuity as a function of overall flux. No obvious trend is apparent; the downturn below 0.3 Jy may be significant, but the sample size for these fainter sources is small. The symbols distinguish the peak-up strategy, with diamonds for a red IRS peak-up (usually on the standard itself), boxes for a blue IRS peak-up (usually using an offset star), and triangles for PCRS peak-ups using a PCRS offset star. The discontinuities do not show any obvious patterns with peak-up strategy.

at higher values of SL1 with respect to LL2, stopping abruptly at a maximum of 1.059 (SL1 over LL2 by 6%). Moving to lower ratios, the distribution trails off steadily. In our sample, the minimum ratio is 0.58 (SL1 under LL2 by 42%).

### 3.2 Investigating Dependencies

Figure 2 shows that the size of the discontinuity does not depend on the flux of the target, at least within the range of our sample. There is evidence of a possible downturn below 0.3 Jy at 14 Jy, and this would be consistent with suggestions from observers who have raised concerns of larger discontinuities in fainter spectra. Unfortunately, the insufficient number of faint sources in this sample prevents any firm conclusions about the discontinuities in faint sources. It is clear that above 0.3 Jy, SL1/LL2 is independent of flux.

Figure 2 uses the symbol type to segregate between red IRS peak-up, blue IRS peak-up, and PCRS peak-up. While the PCRS peak-up sample is too small for meaningful conclusions, there is no evidence that the discontinuity depends on

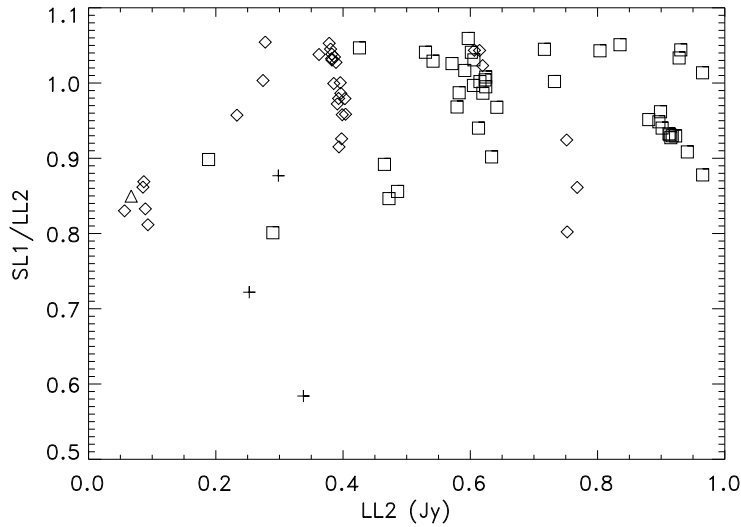


Figure 3 — As Fig. 2, but here the symbols denote the object type. Boxes are for K giants, diamonds for A dwarfs, the solitary triangle for the one solar analog, and plus signs for red objects (galaxies). There is no obvious dependence with the type of star, but all three of the galaxies show discontinuities of 10% or more

the peak-up strategy for IRS peak-ups.

Figure 3 segregates the sample based on object type. The A dwarfs and K giants follow the same distribution. While the sample of galaxies in this database is small (only three), their discontinuities are noticeably different from other sources of the same brightness. All three galaxies show SL1/LL2 ratios under 0.90, and two of the three have the largest discontinuities in the sample.

### 3.3 Individual Sources

It is informative to look more closely at individual sources which have been observed extensively as a part of the calibration program. Figure 4 plots the strength of the discontinuity as a function of flux in both SL1 and LL2 for  $\delta$  UMi (16 observations from Campaign P to 3). Figure 5 provides corroborating results from HD 173511 (11 spectra). The measured flux in SL1 is anti-correlated with the flux in LL2. When the flux drops in one aperture, it rises in the other.

All of the observations of  $\delta$  UMi used red peak-up on the source, while most of the HD 173511 pointings were obtained by observing an offset star with the blue peak-up array. Since the two sets of data show similar anti-correlations, this

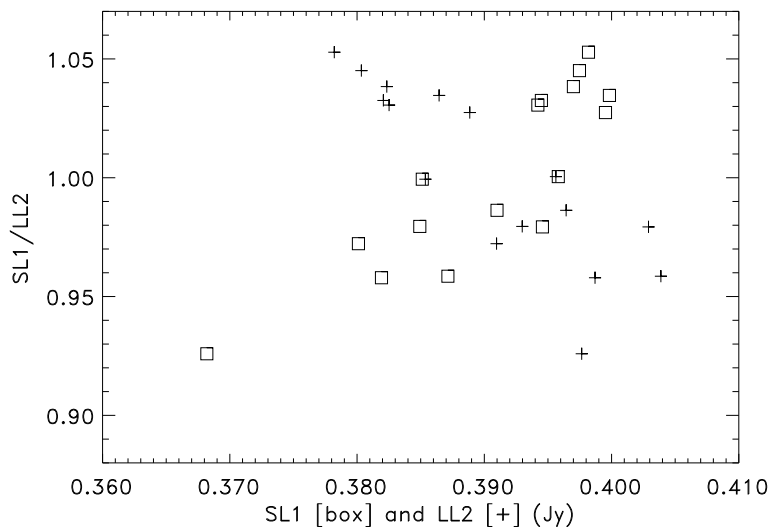


Figure 4 — The ratio SL1/LL2 for  $\delta$  UMi (A1 Vn) as a function of the flux density summed from 14.0 to 14.3  $\mu\text{m}$  in both SL1 (boxes) and LL2 (plus signs). The flux in the two apertures is anti-correlated. When one rises, the other falls. All of the observations of  $\delta$  UMi were obtained using offsets from the red peak-up array

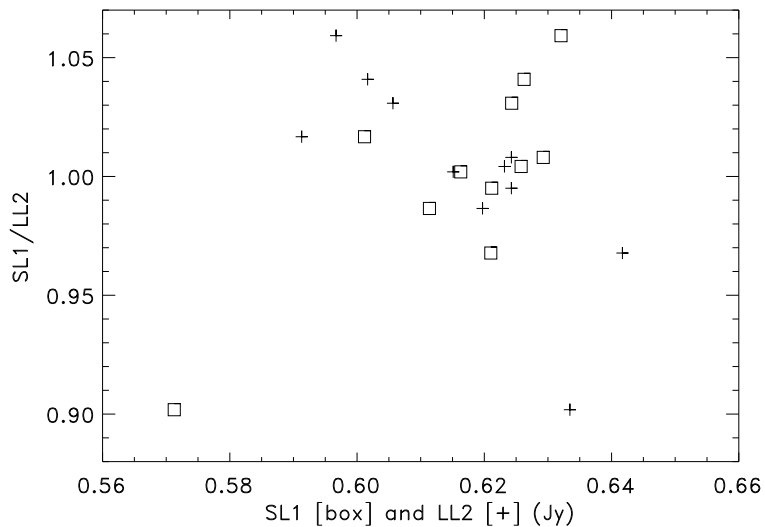


Figure 5 — As Fig. 4, but for HD 173511 (K4 V). The same anti-correlation observed in Fig. 4 is apparent. Most pointings of HD 173511 were obtained by placing an offset star in the blue peak-up array.

behavior cannot be associated with the peak-up strategy.

## 4 Discussion

Qualitatively, the variation in discontinuity from one object to another, and even from one pointing of the same object to another, is consistent with the behavior expected from spectral pointing-induced throughput error (SPITE; see Sloan et al., IRS-TR 03001; Nerenberg & Sloan, IRS-TR 03003). As the telescope moves a target from one aperture to the next, random pointing errors would naturally lead to discontinuities in adjacent spectral segments observed in different apertures. This problem would be exacerbated by the difference in the size between the SL and LL slits.

Applying the same model used in IRS-TR 03001 and 03003 shows that the mean discontinuity of 4% (SL/LL=0.96) corresponds to a  $0''.55$  offset in the dispersion direction. A discontinuity of 9% requires a  $0''.82$  offset in SL. If the discontinuity is 9% in the other sense (SL/LL=1.09), the star would have to be  $3''.21$  from the center of the LL slit.

These pointing errors are much larger than the  $0''.40$   $1\sigma$  errors expected in SL, which raises three possibilities. (1) The actual pointing errors are significantly larger than expected. (2) The model used is producing inaccurate results. (3) Something in addition to pointing is contributing to the discontinuities. There are no independent suggestions of pointing issues with the Spitzer Space Telescope on the scale required to produce the observed discontinuities, so the first possibility seems unlikely if the pointing errors are randomly distributed. The model used a theoretical Airy function convolved with a rectangular slit to estimate the throughput at each wavelength, which involves a number of simplifications. Improving the SPITE model may provide the best means of determining if offsets consistent with the observed pointing behavior can produce the observed discontinuities.

Other factors may also be contributing to the strength of the discontinuities. The behavior of the three red sources in Figure 3 raises the possibility that the discontinuity might be color-dependent. Could this arise from a light leak in LL? Light leaking into LL2 would come from shorter wavelengths, and thus blue sources would be more strongly affected than red sources. A spectrophotometric correction generated from blue sources would correct all LL2 spectra downward at  $14\ \mu\text{m}$ , and this would tend to raise the ratio SL1/LL2, not lower it. Analysis of measurements during in-orbit checkout and science verification have limited any

light leaks into LL to less than 10%. Given that the discontinuities for the three galaxies are as much as 30% greater than typical, it is difficult to see how a light leak even as large as 10% could account for it. Thus, a light leak would produce a discontinuity in an opposite sense to what is typically observed, and it would be too small in any event.

The LL slit is nearly three times as wide as the SL slit, so a given random offset in position would produce a larger SPITE effect in SL than in LL. Thus, if the pointing offsets in LL are approximately the same size as in SL, one would expect the range of observed fluxes in Figures 4 and 5 to be much smaller for LL than SL. This is not the case.

The SL and LL slits are nearly perpendicular to each other. If one of the slits were not mapped to sufficient accuracy, the perpendicular slits could produce an anti-correlation like that shown in Figures 4 and 5. When a given pointing error places the star near the center of one slit, this might move it away from the center of the other slit. If the slits are in fact not mapped with sufficient accuracy, the anti-correlation shown in Figures 4 and 5 would be the first indication of it.

## 5 Conclusion

Analysis of the 86 spectrophotometric calibration AORs obtained in Campaigns P, 1, 2, and 3 reveals that the  $1\sigma$  distribution in discontinuities between SL1 and LL2 is approximately 9%, although the distribution is not Gaussian. This finding will not change if the relative calibration of SL1 and LL2 change.

Using the calibrations described in this report, the mean discontinuity, expressed as a ratio of SL1/LL2, is 0.96, with a maximum of 1.06 and a minimum of 0.58.

The behavior of the discontinuities shows no relation to peak-up strategy, stellar type, or flux (for sources above 0.3 Jy at 14  $\mu\text{m}$ ). There are hints that the discontinuities may be larger for red sources and for fainter sources, but the sample examined here does not contain enough of these sources to allow a stronger conclusion. While the behavior of the discontinuities is qualitatively consistent with SPITE, quantitative agreement is lacking.

The analysis of the sources  $\delta$  UMi and HD 173511, which have been observed multiple times, reveals an anti-correlation between the flux measured in SL1 and LL2 that would not be expected for a randomly distributed sample of offsets from the centers of the two slits.



## **References**

Nerenberg, P.S., & Sloan, G. C. 2003, IRS-TR 03003: Correcting for Spectral Pointing-Induced Throughput Error

Sloan, G. C., Nerenberg, P. S., & Russell, M. R. 2003, IRS-TR 03001: The Effect of Spectral Pointing-Induced Throughput Error on Data from the IRS